

## **Supporting Information**

### **Distinguishing Potassium Channel Resting State Conformations in Live Cells with Environment-Sensitive Fluorescence**

Sebastian Fletcher-Taylor<sup>a,b,‡</sup>, Parashar Thapa<sup>b,‡</sup>, Rebecka J. Sepela<sup>b</sup>, Rayan Kaakati<sup>b,†</sup>, Vladimir Yarov-Yarovoy<sup>b,d</sup>, Jon T. Sack<sup>b,d,\*</sup>, and Bruce E. Cohen<sup>a,c,\*</sup>

<sup>a</sup>The Molecular Foundry and <sup>c</sup>Division of Molecular Biophysics & Integrated Bioimaging, Lawrence Berkeley National Laboratory, Berkeley, CA 94720, United States

<sup>b</sup>Departments of Physiology and Membrane Biology and <sup>d</sup>Anesthesiology and Pain Medicine, University of California, Davis, CA 95616, United States

<sup>‡</sup>S.F-T. and P.T. contributed equally to this work.

\*To whom correspondence may be addressed. Email: [becohen@lbl.gov](mailto:becohen@lbl.gov), [jsack@ucdavis.edu](mailto:jsack@ucdavis.edu)

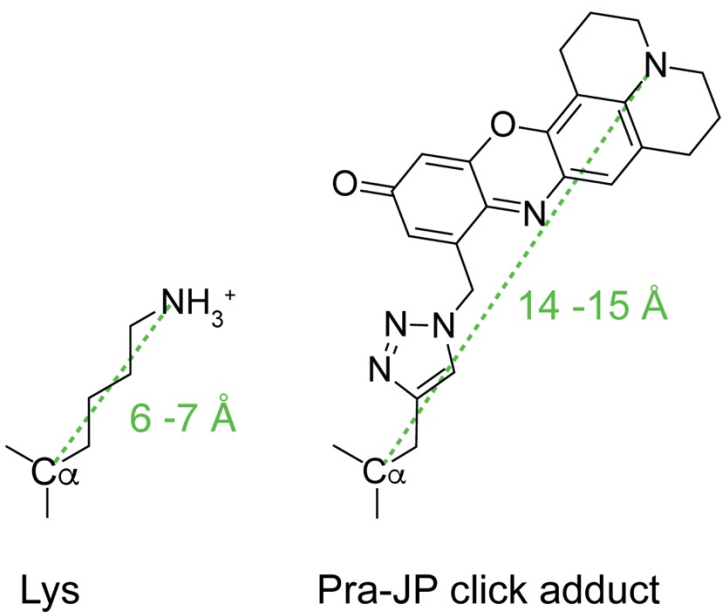


**Figure S1.** Structure and dimensions of JP- $\text{N}_3$  click adduct with Pra sidechain compared to extended Lys sidechain. Distance measurement is from peptide  $\text{C}\alpha$  to furthest point in the chromophore. Distances were calculated with Chem3D (CambridgeSoft).

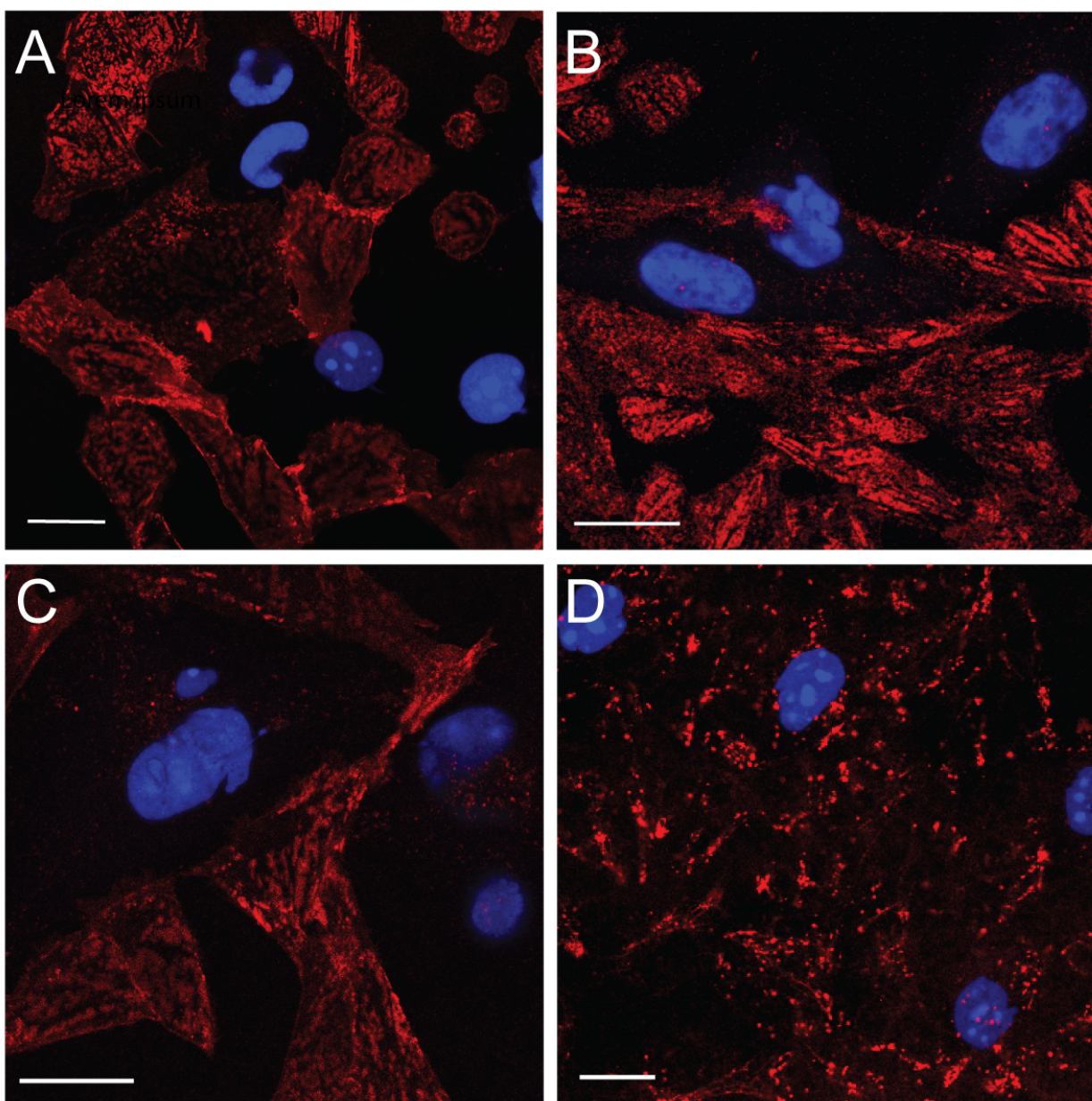


**Figure S2.** Live-cell confocal imaging of GxTX-JP conjugates with Kv2.1-expressing cells. Kv2.1-expressing CHO cells were co-plated with nuclear BFP-expressing CHO cells not expressing Kv2 channels and stained with 100 nM GxTX Pra(JP) conjugates substituted at: (A) Lys10 (B) Ser13 (C) Lys27 and (D) Phe33. Red is JP emission and blue is nuclear BFP emission. Scale bars are 20  $\mu$ m. Lys10, Ser13, and Phe33 conjugates were excited at 594 nm; the Lys27 conjugate was excited at 543 nm.

**Table S1.** Curve-fitting of fluorescence spectra with split pseudo-Voigt functions.

conjugate	membrane potential	fit components	$a_0$	$a_1$ (peak)	$a_2$	$a_3$	$a_4$	$a_5$	$R^2$
JP10 <sup>a</sup>	resting	1	0.973	656.0	16.08	28.68	1.084	0.804	0.990
JP10	resting	1	0.921	654.8	16.98	34.65	0.224	0.876	0.960
JP10	resting	2	0.101	590.4	16.98	34.65	0.224	0.876	0.985
			0.894	655.6	16.98	34.65	0.224	0.876	
JP10	+40 mV	2	0.021	617.6	16.98	34.65	0.224	0.876	0.994
			0.954	651.4	16.98	34.65	0.224	0.876	
JP10	-80 mV	2	0.055	617.1	16.98	34.65	0.224	0.876	0.996
			0.940	652.3	16.98	34.65	0.224	0.876	
JP13 <sup>a</sup>	resting	1	1.022	651.7	18.86	32.85	0.689	1.318	0.992
JP13	resting	1	1.018	649.7	16.98	34.65	0.224	0.876	0.978
JP13	resting	2	0.085	602.5	16.98	34.65	0.224	0.876	0.990
			0.983	650.7	16.98	34.65	0.224	0.876	
JP13	+40 mV	2	0.193	622.2	16.98	34.65	0.224	0.876	0.994
			0.839	653.7	16.98	34.65	0.224	0.876	
JP13	-80 mV	2	0.226	622.5	16.98	34.65	0.224	0.876	0.996
			0.863	654.2	16.98	34.65	0.224	0.876	
JP33 <sup>a</sup>	resting	1	1.012	657.0	15.63	24.84	0.767	1.364	0.996
JP33	resting	1	0.913	655.4	16.98	34.65	0.224	0.876	0.974
JP33	resting	2	0.057	573.0	16.98	34.65	0.224	0.876	0.982
			0.902	655.6	16.98	34.65	0.224	0.876	
JP27 <sup>b</sup>	resting	1	0.915	608.1	16.98	34.65	0.224	0.876	0.991
JP27 (no Kv2)	-80 mV	2	0.527	585.1	16.98	34.65	0.224	0.876	0.945
			0.821	624.5	16.98	34.65	0.224	0.876	
JP27 (no Kv2)	+40 mV	2	0.593	591.7	16.98	34.65	0.224	0.876	0.942
			0.762	628.6	16.98	34.65	0.224	0.876	
JP27	-100 mV	2	0.952	613.0	16.98	34.65	0.224	0.876	0.992
			0.200	642.8	16.98	34.65	0.224	0.876	
JP27	-80 mV	2	0.863	612.2	16.98	34.65	0.224	0.876	0.996
			0.268	637.3	16.98	34.65	0.224	0.876	
JP27	-60 mV	2	0.919	612.9	16.98	34.65	0.224	0.876	0.996
			0.262	642.2	16.98	34.65	0.224	0.876	
JP27	-40 mV	2	0.733	611.2	16.98	34.65	0.224	0.876	0.989
			0.418	635.3	16.98	34.65	0.224	0.876	
JP27	-20 mV	2	0.821	612.1	16.98	34.65	0.224	0.876	0.992
			0.389	638.0	16.98	34.65	0.224	0.876	
JP27	0 mV	2	0.714	611.6	16.98	34.65	0.224	0.876	0.996
			0.497	638.2	16.98	34.65	0.224	0.876	
JP27	+20 mV	2	0.631	610.1	16.98	34.65	0.224	0.876	0.993
			0.606	637.1	16.98	34.65	0.224	0.876	
JP27	+40 mV	2	0.600	609.6	16.98	34.65	0.224	0.876	0.984
			0.666	637.9	16.98	34.65	0.224	0.876	
JP27	+60 mV	2	0.587	609.8	16.98	34.65	0.224	0.876	0.991
			0.655	637.9	16.98	34.65	0.224	0.876	

JP27	+80 mV	2	0.624	609.9	16.98	34.65	0.224	0.876	0.989
			0.644	638.5	16.98	34.65	0.224	0.876	
JP27	+100 mV	2	0.531	610.1	16.98	34.65	0.224	0.876	0.978
			0.649	635.5	16.98	34.65	0.224	0.876	
JP27	-80 mV	1	1.073	616.9	16.98	34.65	0.224	0.876	0.968
JP27	+80 mV	1	1.144	624.6	16.98	34.65	0.224	0.876	0.874
JP-N <sub>3</sub> / toluene	NA	1	1.029	608.0	16.98	34.65	0.224	0.876	0.976

<sup>a</sup>unconstrained (see Methods)

<sup>b</sup>shape parameters ( $a_2-a_5$ ) used as references for JP lineshape

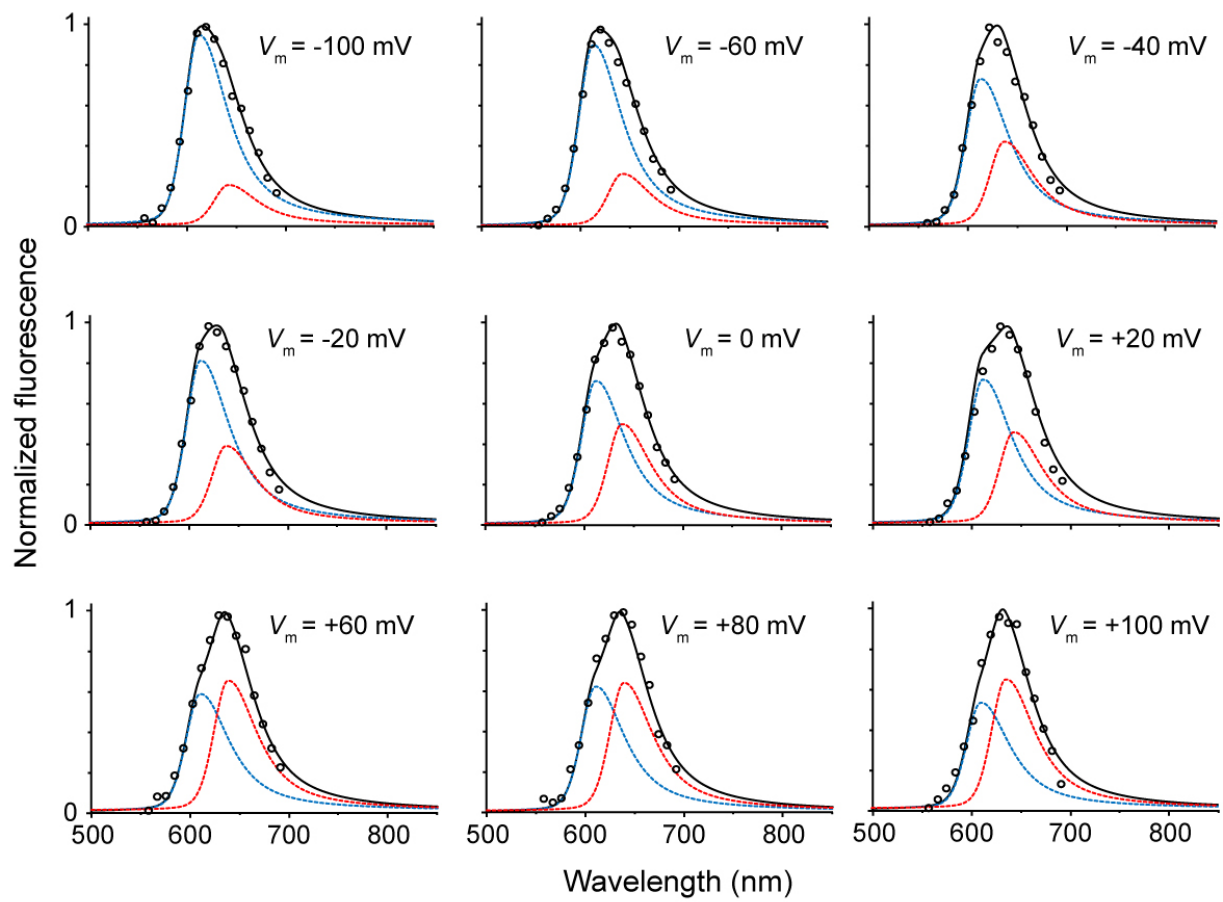


**Figure S3.** Voltage-dependent emission spectra of Lys27Pra(JP) GxTX on Kv2.1-expressing CHO cells under patch clamp. Spectra at -80 mV and +40 mV are shown in Figure 4. Cells were excited at 543 nm, and normalized spectra are fit with 2-component split pseudo-Voigt functions (black) with individual components (blue, red). Split pseudo-Voigt parameters and  $R^2$  fit values are listed in Table S1.

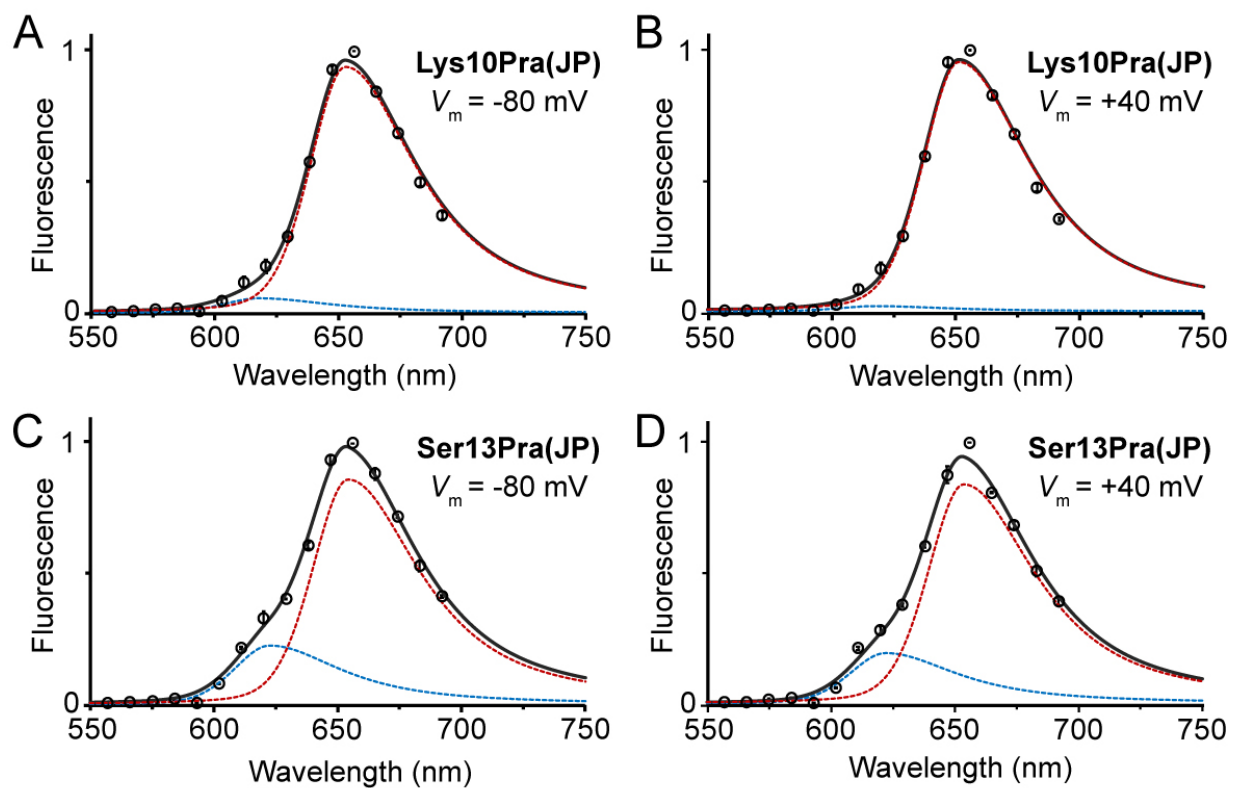


**Figure S4.** Voltage-independent emission of GxTX-JP conjugates on Kv2.1-expressing CHO cells. Normalized fluorescence of JP conjugated at Lys10Pra on cells held at (A) -80 mV or (B) +40 mV. Normalized fluorescence of JP conjugated at Ser13Pra on cells held at (C) -80 mV or (D) +40 mV. All cells were excited at 594 nm, and spectra are fit with 2-component split pseudo-Voigt functions (black) with individual components (blue, red). Split pseudo-Voigt parameters and  $R^2$  fit values are listed in Table S1.

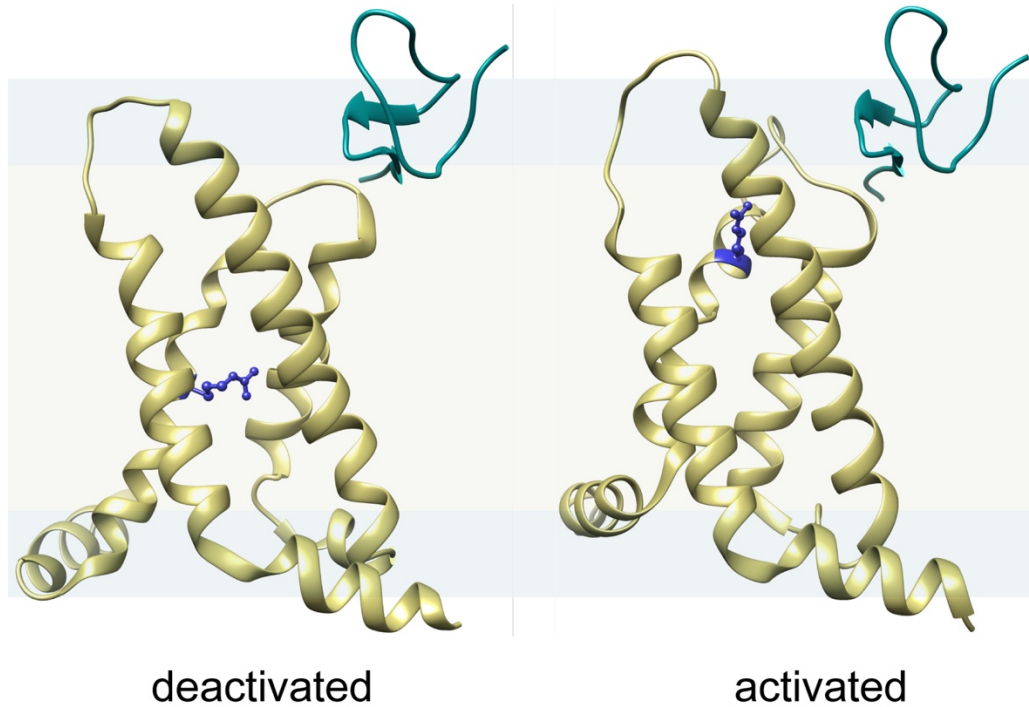


**Figure S5.** CryoEM structures<sup>1</sup> of voltage-sensing domain of channel Nav1.7 in complex with toxin ProTX2, in both deactivated state (PDB ID: 6N4R) and an activated state (PDB ID: 6N4Q). Nav1.7 residues 720 – 853 are shown, with Arg826 highlighted in blue. Deactivated state may be fully or partially resting state.

## **References**

1. Xu, H.; Li, T.; Rohou, A.; Arthur, C. P.; Tzakoniati, F.; Wong, E.; Estevez, A.; Kugel, C.; Franke, Y.; Chen, J.; Ciferri, C.; Hackos, D. H.; Koth, C. M.; Payandeh, J., Structural Basis of Nav1.7 Inhibition by a Gating-Modifier Spider Toxin. *Cell* **2019**, *176* (4), 702-715.e14.